Robert J. Casson, John P. M. Wood, Guoge Han, Thaksaon Kittipassorn, Daniel J. Peet, and Glyn Chidlow

M-type pyruvate kinase isoforms and lactate dehydrogenase a in the mammalian retina: metabolic implications

Investigative Ophthalmology and Visual Science, 2016; 57(1):66-80

M-Type Pyruvate Kinase Isoforms and Lactate Dehydrogenase A in the Mammalian Retina: Metabolic Implications

Robert J. Casson,[1,2] John P. M. Wood,[1,2] Guoge Han,[1,2] Thaksaon Kittipassorn,[2,3] Daniel J. Peet,[3] and Glyn Chidlow[1,2]

[1]Ophthalmic Research Laboratories, Hanson Institute Centre for Neurological Diseases, Adelaide, South Australia, Australia
[2]South Australian Institute of Ophthalmology, University of Adelaide, Adelaide, South Australia, Australia
[3]School of Biological Science, University of Adelaide, Adelaide, South Australia, Australia

Correspondence: Robert J. Casson, South Australian Institute of Ophthalmology, Adelaide, SA 5000, Australia;
robert.casson@adelaide.edu.au.

Submitted: August 15, 2015
Accepted: December 2, 2015

Citation: Casson RJ, Wood JPM, Han G, Kittipassorn T, Peet DJ, Chidlow G. M-type pyruvate kinase isoforms and lactate dehydrogenase A in the mammalian retina: metabolic implications. *Invest Ophthalmol Vis Sci*. 2016;57:66–80. DOI:10.1167/iovs.15-17962

Purpose. Like cancer cells, photoreceptor cells produce lactate aerobically, requiring lactate dehydrogenase A (LDH-A). Cancer cells also use glycolytic intermediates for biosynthesis. The molecular switch controlling glycolytic flow is thought to be an isoenzyme of pyruvate kinase (PKM2). Here, we determined the expression and localization of PKM2 and LDH-A in mammalian retina and make comparisons with the brain.

Methods. Single- and double-labeling immunohistochemistry for PKM2, pyruvate kinase M1 (PKM1), and LDH-A were performed using retinal sections from C57BL/6 mice, Sprague-Dawley rats, rabbits, marmosets, and humans. Pyruvate kinase M1 and PKM2 mRNA and protein expression levels were quantified in rodent retina and brain by using qPCR and immunoblotting. The quaternary forms of PKM2 in rat retina were also determined.

Results. Pyruvate kinase M2 was present in some glial cells and rod and cone photoreceptors in the retina of all species but was exclusively localized to glia in the brain. Pyruvate kinase M1 was confined to neurons in the retina and brain. Lactate dehydrogenase A was principally found in photoreceptors and inner portion of the avascular rabbit retina. Western blotting and qPCR confirmed high levels of PKM2 and LDH-A in the retina. There was a 6- to 9-fold greater expression of PKM2 mRNA in the rodent retina than in the brain. Both the dimeric (inactive, biosynthesis-driving form) and the active tetrameric (glycolytic-driving) forms of PKM2 were present in retina but not in brain.

Conclusions. Mammalian photoreceptors contain dimeric and tetrameric PKM2 and LDH-A. This is consistent with the ability to switch between energy production and biosynthesis like a proliferating tissue, possibly due to demands of opsin synthesis.

Keywords: lactate dehydrogenase, metabolism, optic nerve, PKM2, retina

Retinal photoreceptors have a metabolism that is in some ways more reminiscent of a neoplastic cell than a central nervous system neuron.[1] That is, they face prodigious energy demands to maintain their "dark current"[2] and large biosynthesis requirements due to the rapid shedding and renewal of their outer segments.[3] Like cancer cells, photoreceptor cells rely heavily on both glycolysis and oxidative phosphorylation to meet energy demands, and like cancer cells, isolated retina has a high glycolytic flux and lactate production even in the presence of oxygen, a phenomenon known as aerobic glycolysis or the Warburg effect.[4,5] Limited evidence indicates that the retinal Warburg effect is actually predominantly localized to photoreceptors with minimal contribution from the inner retina.[4,6–8] Relatively high levels of lactate production by retinal cells in the presence of oxygen define the presence of the Warburg effect but are difficult to measure in vivo. It is also difficult to define the specific cellular source of lactate production. A surrogate marker in vivo, thus, is the presence of lactate dehydrogenase (LDH), consisting of the subunits LDH-A and LDH-B. The LDH-A isoform catalyzes the conversion of pyruvate to lactate, reforming nicotinamide adenine dinucleotide (NAD^+) to support ongoing glycolysis. Lactate dehydrogenase A is used as a cancer biomarker and is under consideration as a therapeutic target for cancer.[9] To our knowledge, the cell-specific localization of LDH-A in the retina has never been reported.

Glycolysis in cancer cells, in addition to providing energy, is also able to provide anabolic building blocks for cellular proliferation.[10] The requirement of a proliferating cell for both glycolysis-derived biosynthesis and adenosine triphosphate (ATP) production in the presence of oxygen has been termed a "metabolic budget system" (MBS).[11] Pyruvate kinase (PK) catalyzes the final step of glycolysis, converting phosphoenolpyruvate to pyruvate. The molecular switch responsible for the MBS is an isoenzyme of PK known as PKM2.[11] An alternative isoform, PKM1, is found in nonproliferating tissue.[12] Structurally, both PKM1 and PKM2 exist as homotetramers, configurations that favor glycolytic flux. Pyruvate kinase M2, however, unlike PKM1, is under allosteric control by the upstream glycolytic intermediate fructose-1,6-biphosphate[12] and the amino acid serine.[13] Allosteric modulation causes the PKM2 tetramer to dissociate to a dimer. Dimeric PKM2 is much less

efficient at converting phosphoenolpyruvate to pyruvate, and its presence therefore slows the rate of glycolytic flux; the resultant accumulation of upstream glycolytic intermediates can then be used for anabolic reactions. The presence of a dimeric form of PKM2 within a cell, therefore, implies a reduced rate of glycolysis and an increased level of biosynthesis derived from glycolytic intermediates. Recent data indicate that rodent photoreceptors contain PKM2,[14] and intriguingly, that anti-PKM2 antibodies are present in the serum of individuals with age-related macular degeneration.[15]

In order to advance our understanding of the unique metabolism of the retina, a detailed characterization of the levels of expression, cellular distribution, and species correspondence among PKM1, PKM2, and LDH-A in the retina versus that in brain is needed. In this study, we investigated expression of PKM1, PKM2, and LDH-A in the retina, optic nerve, and cerebral cortex of mouse, rat, rabbit, common marmoset (*Callithrix jacchus*), and human.

Materials and Methods

Animals and Tissue Processing

This study was approved by the SA Pathology/Central Heath Network (CHN) Animal Ethics Committee (Adelaide, Australia) and conformed to the Australian Code of Practice for the Care and Use of Animals for Scientific Purposes, 2004, and with the Association for Research in Vision and Ophthalmology statement for the use of animals in vision and ophthalmic research. Adult Sprague-Dawley rats (approximately 250 g) and C57BL/6 mice were housed in a temperature- and humidity-controlled room with a 12L:12D cycle (lights on 7 AM) and were provided with food and water ad libitum. Light-adapted rodents were killed by transcardial perfusion with physiological saline under deep anesthesia between 2 and 9 PM. Both eyes with optic nerves attached were enucleated immediately. The brain was also taken when necessary. Rabbit eyes were obtained locally and fixed within 30 minutes of the animal's death.

Human ocular tissue for analysis was obtained from the Eye Bank of South Australia, Flinders Medical Centre (Adelaide, Australia), following guidelines of the Southern Adelaide Clinical Human Research Ethics Committee; all tissues had been screened to ensure there was no underlying ocular disease, and all were from Caucasian donors 50 to 65 years of age. Following ethical approval from the SA Pathology/CHN Animal Ethics Committee (Adelaide, Australia), we obtained ocular tissue from three adult marmosets (*Callithrix jacchus*) belonging to the colony housed at the Queen Elizabeth Hospital (South Australia, Australia) that were being euthanized. We are grateful to Toby Coates for participating in this tissue-sharing initiative, which has obvious benefits from an ethical perspective.

There was no consistent orientation of rodent, primate, or human globes with regard to nasal-temporal or dorsal-ventral quadrants of the retina analyzed. Sections were typically taken at the level of the optic nerve head and, hence, consisted of at least two quadrants. We cannot categorically rule out expression differences between different regions of the retina in any species; however, no such differences were apparent in any of our examinations.

Globes and optic nerves that were subsequently used for immunohistochemistry were fixed by immersion in Davidson's solution for 24 hours and then transferred to 70% ethanol until processing. Davidson's solution (2 parts formaldehyde [37%], 3 parts 100% ethanol, 1 part glacial acetic acid, and 3 parts water) is the preferred fixative for whole eyes as it provides optimal tissue morphology while avoiding retinal detachment. Brains were immersion-fixed in 10% buffered formalin until processing. Following fixation, the brain was positioned in a Kopf rat brain blocker (Kopf Instruments, Tujunga, CA, USA), and 2-mm coronal slices were taken starting from the dorsal and proceeding to the caudal portion of the brain. Brain slices along with the globe and optic pathway were then processed for routine paraffin-embedded sectioning. Globes were embedded sagittally and optic nerves longitudinally. In all cases, 4-μm sections were cut.

Immunohistochemistry

Colorimetric immunohistochemistry was performed as previously described.[16–18] Briefly, tissue sections were deparaffinized, endogenous peroxidase activity was blocked, and high-temperature antigen retrieval was performed. Subsequently, sections were incubated in primary antibody (Supplementary Table S1), followed by consecutive incubations with biotinylated secondary antibody and streptavidin-peroxidase conjugate. Color development was achieved using NovaRed (Sao Paolo, Brazil) substrate kit.

For double-labeling fluorescent immunohistochemistry, visualization of one antigen was achieved using a 3-step procedure (primary antibody, biotinylated secondary antibody, streptavidin-conjugated AlexaFluor 488 or 594 [Thermo Fisher Scientific, Waltham, MA, USA]), and the second antigen was labeled by a 2-step procedure (primary antibody, secondary antibody conjugated to AlexaFluor 488 or 594). Sections were prepared as described above and then incubated overnight at room temperature in the appropriate combination of primary antibodies. On the following day, sections were incubated with the appropriate biotinylated secondary antibody for the 3-step procedure plus the correct secondary antibody conjugated to AlexaFluor 488 or 594 for the 2-step procedure, followed by streptavidin-conjugated AlexaFluor 488 or 594. Sections were then mounted using antifade mounting medium and were examined using confocal fluorescence microscopy.

Western Blotting

Western blotting was performed as previously described.[17] Briefly, tissue extracts were sonicated in homogenization buffer, diluted with an equal volume of sample buffer, and boiled for 3 minutes. Electrophoresis was performed using 10% denaturing polyacrylamide gels. After proteins were separated, they were were transferred to polyvinylidene fluoride membranes for immunoprobing. Membranes were incubated consecutively with the appropriate primary antibody (Supplementary Table S1), biotinylated secondary antibody, and streptavidin-peroxidase conjugate. Color development was achieved using 3-amino-9-ethylcarbazole. Detection of β-actin or glyceraldehyde-3-phosphate dehydrogenase (GAPDH) was assessed in all samples as a positive gel-loading control.

Determination of oligomerization status for PK isoforms was undertaken by chemically cross-linking individual monomeric subunits in tissue homogenates as follows: Tissues were solubilized by sonication in 100 mM sodium phosphate buffer, pH 7.4, plus 150 mM NaCl, to a final concentration of 10 μg of protein/μL; each sample was divided into 2 tubes containing a equal volumes of the homogenate. The cross-linking agent disuccinimidyl suberate (DSS) was added to one tube from each sample to a final concentration of 1 mM. Addition of an equal volume of vehicle to the second tube from each sample served as the non–cross-linked control. All samples were incubated at 37°C for 1 hour, and then free DSS was quenched by addition of 1/5 volume of 1 M Tris-HCl (pH 7.5). The protease inhibitor phenyl methyl sulphonyl fluoride was added

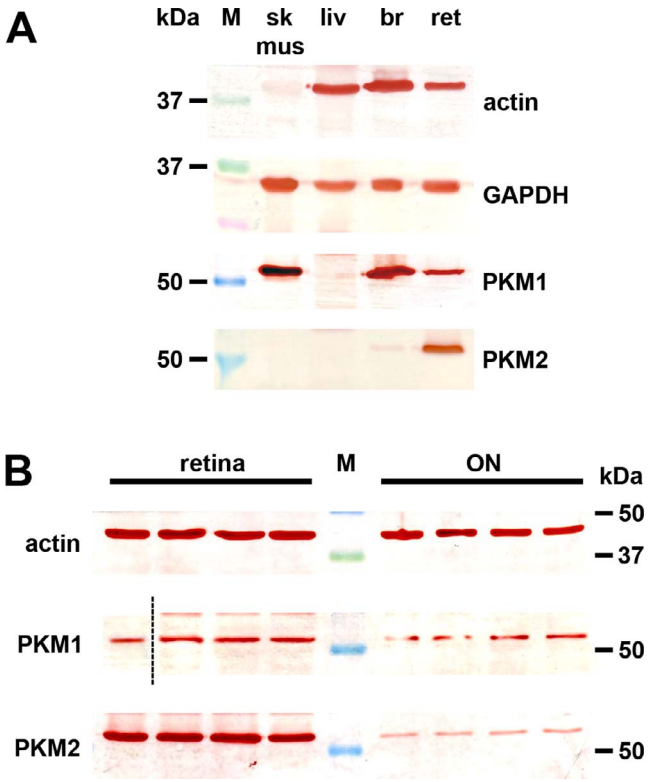

FIGURE 1. Western blot analysis of PKM1 and PKM2 expression in mouse tissues. (**A**) Skeletal muscle (sk mus), liver (liv), brain (br), and retina (ret) tissue extracts were probed for actin, GAPDH, PKM1, and PKM2. Note the absence of actin and PKM2 in skeletal muscle, the absence of PKM1 and PKM2 in liver, and the low level of PKM2 in brain. (**B**) Evaluation of PKM1 and PKM2 expression in retina (*lanes* 1–4) and optic nerve (*lanes* 6–9) from tissue extracts obtained from four different mice. Pyruvate kinase M1 and PKM2 are detectable in all samples but in greater amounts in the retina. The *dotted line* indicates that the first sample was not run in the adjacent lane. M, molecular weight markers.

to a final concentration of 100 μM, and an equal total volume of sample buffer (62.5 mM Tris-HCl, pH 7.4, containing 4% sodium dodecyl sulfate [SDS], 10% glycerol, 10% β-mercaptoethanol, and 0.002% bromophenol blue) was added before all samples were heated to 80°C for 10 minutes. Proteins were resolved on 6% SDS-PAGE gels, and Western blots for different PK isoforms were prepared as described above.

Real-Time RT-PCR

Reverse transcription (RT) polymerase chain reaction (RT-PCR) studies were carried out as described previously.[19] Briefly, entire retinas and optic nerves were dissected, total RNA was isolated, and first-strand cDNA was synthesized from DNase-treated RNA. Real-time PCR reactions were carried out in 96-well optical reaction plates by using the cDNA equivalent of 20 ng of total RNA for each sample in a total volume of 20 μL containing 1× SYBR Green PCR Master Mix (Bio-Rad, Gladesville, Australia) and forward and reverse primers. Thermal cycling conditions were 95°C for 3 min and 40 cycles of amplification at 95°C for 12 seconds, annealing temperature (Supplementary Table S2) for 30 seconds and 72°C for 30 seconds. After the final cycle of the PCR, primer specificity was checked by the dissociation (melting) curve method. In addition, specific amplification was confirmed by electrophoresis of PCR products on 3% agarose gels. PCR assays were performed using the IQ5 iCycler machine (Bio-Rad), and all samples were run in duplicate. Threshold cycles were calculated using IQ5 iCycler software (Bio-Rad). All values were normalized using the endogenous reference gene GAPDH, and results are means ± standard error of the mean (SEM). Primer pairs (Supplementary Table S2) were designed from sequences contained in the GenBank database, using the primer design software Primer 3 (Whitehead Institute for Biomedical Research; http://bioinfo.ut.ee/primer3-0.4.0/primer3/, in the public domain) and were selected to amplify sequences that spanned at least 1 intron. Primer sequences were analyzed for melting temperature (T_m) and secondary structure and primer-dimer formation by using NetPrimer analysis software (http://www.premierbiosoft.com/netprimer, in the public domain; Premier Biosoft, Palo Alto, CA, USA) and verified for their specificity to the target sequence. Results showed that all mRNAs were amplified with high efficiency and linearity during RT-PCR. Mean amplification efficiencies, as determined by plotting cycle threshold as a function of initial cDNA quantity, ranged from 1.9 to 2.0.

Antibody Characterization

Full details of all antisera and antibodies used are shown in Supplementary Table S1. Validation of antibodies to PKM1, PKM2, and LDH-A are detailed in *Results*. Validation of antibodies to β-actin, GAPDH, calretinin, PKCα, and glutamine synthetase are detailed in Supplementary Materials and Methods S1.

RESULTS

PKM1

Validation of Antibodies. All antibodies were validated prior to use. Three commercial antibodies, raised against peptides corresponding to the human PKM1 sequence (Supplementary Table S1) clearly recognized a protein of the expected size (~60 kDa) by Western blotting in mouse skeletal muscle (positive control tissue), brain, retina, and optic nerve but not in liver (negative control tissue). All antibodies provided high signal-to-noise cell-specific immunolabeling in mouse, monkey, and human tissue sections, including positive labeling in extraocular muscle, whereas incubation with preimmune serum alone elicited no labeling. The patterns of immunolabeling of the three antibodies were almost indistinguishable (compare Figs. 1 and 2 for data generated using the antibody from Cell Signaling [Cell Signaling Technology, Inc., Danvers, MA, USA] with data in Supplementary Fig. S1, which features data produced by antibodies from Proteintech [Proteintech Group, Inc., Chicago, IL, USA] and Novus [Novus Biologicals, Littleton, CO, USA]). Thus, it could be concluded that in mouse, marmoset, and human tissues, the data generated were specific to PKM1. Of note, PKM1 antibodies failed to elicit the expected band by Western blotting using rat samples; moreover, no specific staining was detectable in rat tissue sections (data not shown). The explanation for the lack of reactivity of the PKM1 antibodies in rat tissue almost certainly resides in the composition of the single exon that differentiates the PKM1 from the PKM2 isoform. Human, marmoset, and mouse display a high degree of similarity in this exon, but the rat sequence is more divergent.

mRNA and Protein Expression and Immunolocalization. Pyruvate kinase M1 was expressed in high amounts in the brain and retina of mice and rats, with cycle thresholds (C_T) of 17 to 18 cycles, compared to approximately 16 cycles for the housekeeping (and fellow glycolytic) gene GAPDH. There was an approximately 2.5-fold greater expression of

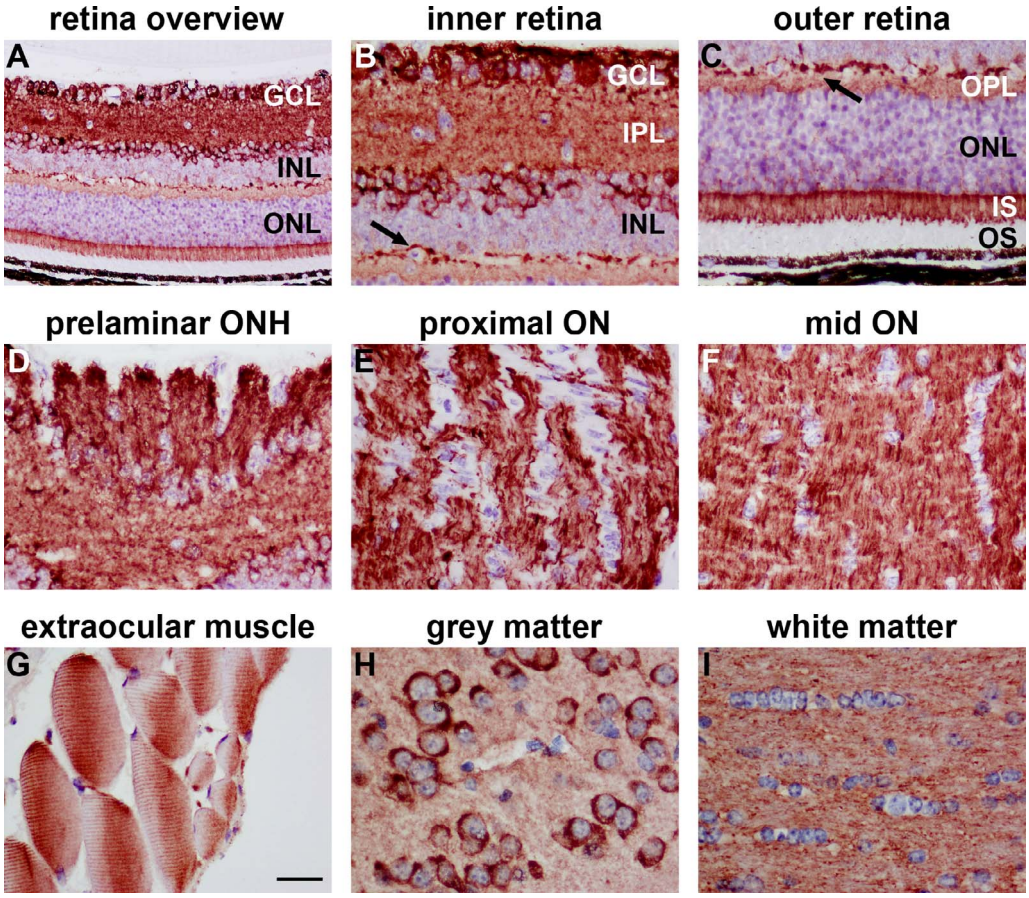

Figure 2. Representative images of PKM1 immunolabeling in mouse tissues. In the retina, positive labeling for PKM1 is localized principally to the inner retina, notably the IPL and populations of cells in the GCL and inner part of the INL (**A**, **B**). In the outer retina, PKM1 is restricted to putative axons in the OPL (*arrow*) and to photoreceptor inner segments (**A**, **C**). Pyruvate kinase M1 is robustly associated with RGC axons in the nerve fiber layer of the retina (**D**) and the optic nerve (**E**, **F**). Pyruvate kinase M1 is also expressed by extraocular muscle (**G**). In the brain, PKM1 is associated with neurons in gray matter (**H**) and axon bundles in white matter (**I**). *Scale bars*: 50 μm (**A**), 25 μm (**B**–**I**). IS, inner segments; ON, optic nerve; ONH, optic nerve head; ONL, outer nuclear layer; OS, outer segments.

PKM1 mRNA in cerebral cortex than in retina when normalized to GAPDH (Table 1). Consistent with this pattern, PKM1 protein, as detected by Western blotting, was more highly expressed in cortex than in retina (Fig. 1A). Analysis of retina and optic nerve samples from four mice revealed similar PKM1 expression in all samples (Fig. 1B).

By immunohistochemistry, PKM1 was principally localized to the inner retina of the mouse, specifically to populations of cells in the ganglion cell layer (GCL) and the inner part of the inner nuclear layer (INL), together with dendritic connections in the inner plexiform layer (IPL) (Fig. 2). In the outer retina, PKM1 immunostaining was evident in the outer plexiform

Table 1. Levels of PKM1, PKM2, and LDH-A mRNAs in Retina and Cortex of Rats and Mice

Gene	Tissue	GAPDH C_T	Target Gene C_T	ΔC_T*	mRNA Level†
PKM1 mouse	Retina	16.5 ± 0.4	18.7 ± 0.5	2.2 ± 0.1	0.23 ± 0.02
	Cortex	16.4 ± 0.1	17.2 ± 0.2	0.9 ± 0.1	0.57 ± 0.04
PKM1 rat	Retina	16.2 ± 0.2	18.4 ± 0.3	2.2 ± 0.1	0.24 ± 0.02
	Cortex	17.4 ± 0.4	18.2 ± 0.5	0.8 ± 0.1	0.57 ± 0.04
PKM2 mouse	Retina	16.5 ± 0.4	17.2 ± 0.5	0.7 ± 0.1	0.64 ± 0.02
	Cortex	16.4 ± 0.1	20.4 ± 0.1	4.0 ± 0.1	0.07 ± 0.003
PKM2 rat	Retina	16.2 ± 0.2	17.3 ± 0.2	1.1 ± 0.1	0.48 ± 0.03
	Cortex	17.4 ± 0.4	21.2 ± 0.3	3.8 ± 0.1	0.08 ± 0.01
LDH-A mouse	Retina	16.5 ± 0.4	18.6 ± 0.3	2.1 ± 0.1	0.26 ± 0.02
	Cortex	16.4 ± 0.1	19.8 ± 0.1	3.4 ± 0.1	0.10 ± 0.003
LDH-A rat	Retina	16.2 ± 0.2	17.8 ± 0.2	1.6 ± 0.1	0.35 ± 0.03
	Cortex	17.4 ± 0.4	20.3 ± 0.6	2.9 ± 0.2	0.15 ± 0.01

C_T, cycle threshold.
* ΔC_T, target gene C_T = GAPDH C_T.
† Target mRNA level was expressed relative to that of GAPDH, where $n = 6$.

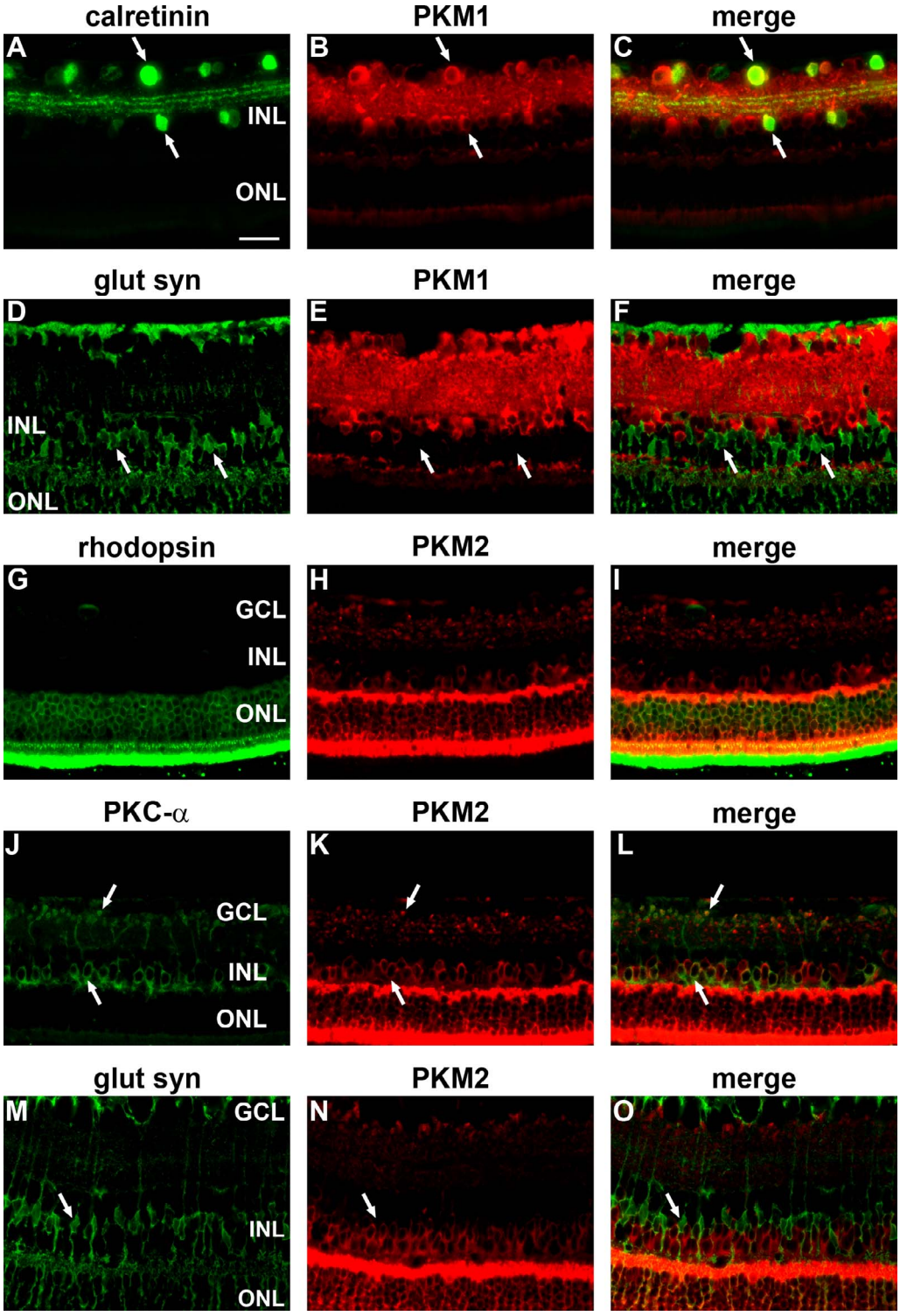

Figure 3. Double labeling immunofluorescence of PKM1 and PKM2 in mouse retina. Pyruvate kinase M1 colocalizes with some calretinin-positive neurons in the GCL and INL ([**A–C**] *arrows*). In contrast, PKM1 is not expressed by glutamine synthetase-positive Müller cells ([**D–F**] *arrows*). Pyruvate kinase M2 colocalizes with the rhodopsin labeling of photoreceptors (**G–I**). Pyruvate kinase M2 also colocalizes with some PKCα-positive bipolar cell bodies in the INL and their terminals adjacent to the GCL ([**J–L**] *arrows*). As with PKM1, there is no obvious association of PKM2 with glutamine synthetase-positive Müller cells ([**M–O**] *arrows*). *Scale bar*: 25 μm.

layer (OPL), in a location consistent with horizontal cell synapses, and in photoreceptor inner segments (Fig. 2). Pyruvate kinase M1 was robustly associated with retinal ganglion cell (RGC) axon bundles throughout the nerve fiber layer of the retina and the optic nerve, but there was no discernible expression of PKM1 by optic nerve glia (Fig. 2). Double-labeling experiments revealed that PKM1 colocalized with calretinin in the GCL and INL (Fig. 3). Calretinin-positive neurons are reported to be subsets of both amacrine cells and RGCs.[20] Pyruvate kinase M1 expression by RGCs and their

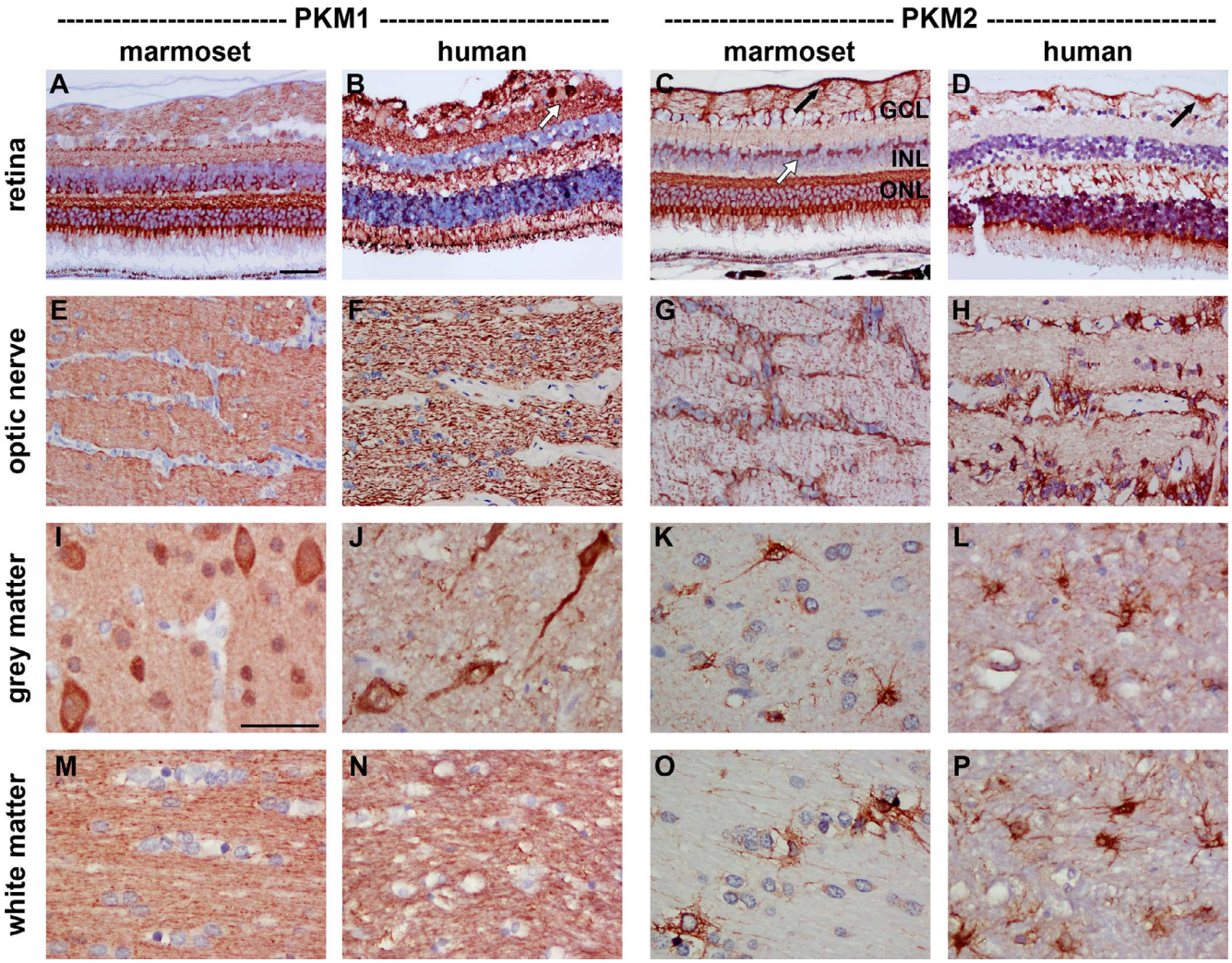

Figure 4. Representative images of PKM1 and PKM2 immunolabeling in marmoset and human tissues. In the marmoset and human retina, PKM1 is widely distributed, with positive labeling evident in the GCL (*arrow*), INL, and ONL, both plexiform layers, and nerve fiber layer (**A**, **B**). Pyruvate kinase M1 labels axon bundles in marmoset and human optic nerve (**E**, **F**). In marmoset and human brain, PKM1 is associated with neurons in gray matter (**I**, **J**) and axon bundles in white matter (**M**, **N**). In marmoset and human retina, PKM2 is restricted to photoreceptors (**C**, **D**), astrocytes (*black arrows*), and Müller cells (*white arrow*). In marmoset and human optic nerve (**G**, **H**), gray matter (**K**, **L**), and white matter (**O**, **P**), PKM2 is associated with astrocytes. *Scale bars*: 50 μm (**A**–**H**), 25 μm (**I**–**P**).

axons, as well as that of amacrine cells, was confirmed by colocalization with β_3-tubulin, Brn3a, and parvalbumin (data not shown). Notably, PKM1 did not colocalize with glutamine synthetase (Fig. 3) or S100 (data not shown), indicating a lack of discernible expression by Müller cells and astrocytes. In the mouse brain, PKM1 was localized to neurons in gray matter and axon bundles in white matter (Fig. 2). As in the retina and optic nerve, there was no observable expression of PKM1 by glial cells (Fig. 2).

In marmosets and humans, Western blotting (Supplementary Fig. S2) and immunohistochemistry (Fig. 4) indicated expression of PKM1 in retina, optic nerve, and brain. The distribution of PKM1 was fundamentally analogous to that observed in the rodent, with positive labeling evident in neurons and their axons, but not in glia. It should be noted, however, that in the marmoset and human retina, unlike the rodent retina, PKM1 distribution was more widespread, encompassing neurons in the inner and outer part of the INL as well as photoreceptor somata and inner segments.

Pyruvate Kinase M1

Validation of Antibodies. Initial analysis of antibodies from two different commercial sources demonstrated that, although both of the antibodies detected a band of approximately the expected size of 60 kDa, the antibodies detected distinct bands of slightly different apparent size (Supplementary Fig. S3). Hence the Novus antibody (Supplementary Table S1) was not used in this study, but two antibodies from Cell Signaling (Supplementary Table S1) were used for subsequent experiments as they were generated using peptides specific for the region of PKM2 divergent from PKM1, and specificity was independently verified using short interfering RNA (siRNA)-based knockdown of PKM2.[21] Further analysis showed the two Cell Signaling antibodies recognized a protein of the expected size by Western blotting in testis (positive control tissue) (Supplementary Fig. S4) and retina but not in liver or skeletal muscle (negative control tissues). Both of the antibodies provided high signal-to-noise, cell-specific immunolabeling in mouse, rat, rabbit, monkey, and human tissue sections. Neither of the antibodies elicited positive labeling in extraocular

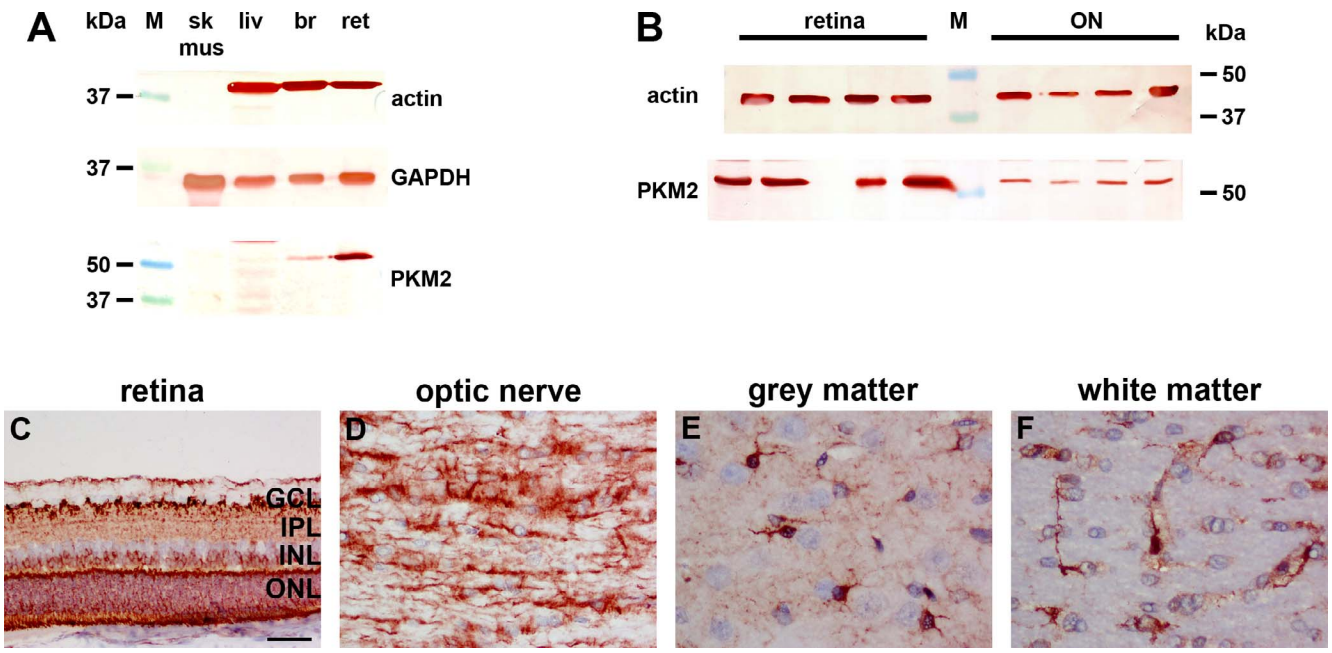

Figure 5. Analysis of PKM2 expression in rats. (**A**) Western blot analysis of PKM2 expression in rat tissues. Skeletal muscle (sk mus), liver (liv), brain (br), and retina (ret) tissue extracts probed for actin, GAPDH, and PKM2. Note the absence of actin and PKM2 in skeletal muscle, absence of PKM2 in liver, and low level of PKM2 in brain. (**B**) Evaluation of PKM2 expression in retina (lanes 1–4) and optic nerve (lanes 6–9) tissue extracts obtained from four different rats. Pyruvate kinase M2 is detectable in all samples but in greater amounts in the retina. (**C–F**) Representative images of PKM2 immunolabeling in rat tissues. In the retina, positive labeling for PKM2 is localized to a population of cells in the outer part of the INL and to photoreceptor cell bodies and their segments (**C**). In addition, PKM2 is associated with terminals in the IPL and to astrocytes (**C**). In the optic nerve, PKM2 is localized to cells with the morphology of astrocytes (**D**). In the brain, PKM2 is associated with astrocytes in gray matter (**E**) and white matter (**F**). *Scale bars*: 50 μm (**A**), 25 μm (**B–D**).

muscle (negative control), and incubation with preimmune serum alone also elicited no labeling. Patterns of immunolabeling of the two antibodies were indistinguishable. Thus, it can be concluded that, in all species, the data generated were specific to PKM2 (Figs. 1, 4, 5, 6, 7, 8).

mRNA and protein expression and immunolocalization. Relative to GAPDH expression, there was 6-fold greater expression of PKM2 mRNA in rat retina and 9-fold greater expression in mouse retina than that in cortex (Table 1). The abundance of the PKM2 transcript in the retina was evident by the low C_T findings in both mouse and rat ($C_T \sim 17$), less than 1 C_T greater than GAPDH. Consistent with mRNA data, PKM2 protein, as detected by Western blotting, was highly expressed in retinal samples and barely detectable in cortex (Figs. 1A, 5A). Analysis of retina and optic nerve samples from four rats and mice revealed PKM2 expression in all samples but much fainter bands in optic nerve samples (Figs. 1B, 5B).

Distribution of PKM2 in rodent retina contrasted markedly with that of PKM1. In both rats (Fig. 5) and mice (Fig. 6), robust labeling of PKM2 was evident in photoreceptor cell bodies and their inner and outer segments. Double-labeling experiments showed that PKM2 colocalized with rhodopsin (Fig. 3). Pyruvate kinase M2 was also associated with a population of cells in the outer part of the INL, in the histoanatomical location of bipolar cells, together with terminals in the IPL. Confirmation that these cells were bipolar cells was achieved by successful colocalization of PKM2 with the optic nerve bipolar cell marker PKCα (Fig. 3). Pyruvate kinase M2 was not associated with RGC axons in the nerve fiber layer of the retina nor in the optic nerve but was localized to astrocytes. Analogous to PKM1, PKM2 did not colocalize with glutamine synthetase (Fig. 3) or S100 (data not shown) in the INL, indicating a lack of discernible expression by Müller cells. Importantly, 5-fold dilution of the PKM2 antibody eliminated all labeling, with the exception of that associated with photoreceptors, suggesting that photoreceptors express higher levels of PKM2 than other retinal cells (data not shown). In the rodent brain, PKM2 was exclusively associated with astrocytes, in both gray and white matter (Figs. 5, 6).

It has been suggested that PKM2 expression in the retina is restricted to photoreceptors.[14] To corroborate our finding of PKM2 expression by nonrod photoreceptors, we analyzed 8-week-old rd1 mice, which feature completely degenerated rod photoreceptors but some residual M-, L-, and S-cone photoreceptors (Supplementary Fig. S5). First, we probed retinal extracts from rd1 mice and age-matched C57BL/6 (wild-type) mice for rhodopsin kinase, calretinin, PKM1, and PKM2 by Western blotting. Compared with wild-type retinas, there was an absence of rhodopsin kinase, as expected, and a lower but still clearly detectable amount of PKM2 in *rd1* retinas (Fig. 7A). Subsequently, we performed immunohistochemistry using tissue sections and showed, as expected, unambiguous PKM2 labeling of bipolar cells, astrocytes, and probably cones in both rd1 and wild-type retinas (Figs. 7B, 7C). The rod-dominant rodent retina, however, is not ideal for demonstrating that cones express PKM2. Moreover, although residual cones are present within the rd1 retina, they may well not be metabolically normal. Thus, to firmly establish whether cones express PKM2, we used primate retina (see below).

In marmosets and humans, Western blotting (Supplementary Fig. S2) and immunohistochemistry (Fig. 4) indicated expression of PKM2 in retina, optic nerve, and brain. Distribution of PKM2 was broadly similar to that observed in rodent, with positive labeling in the retina associated with photoreceptors and astrocytes and in the optic nerve and brain exclusively with astrocytes. Nevertheless, some differences were apparent with regard to retinal expression compared with that in rodents: first, in the marmoset, PKM2 was not

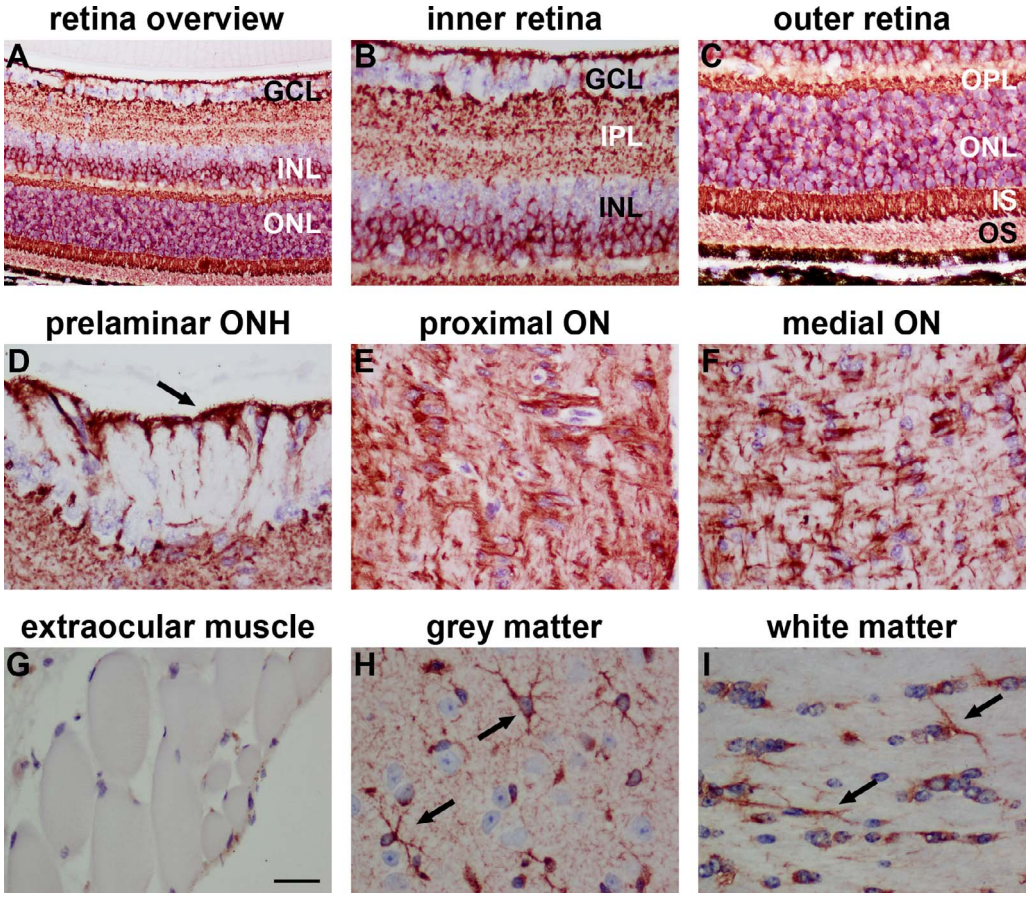

Figure 6. Representative images of PKM2 immunolabeling in mouse tissues. In the retina, positive labeling for PKM2 is localized to a population of cells in the outer part of the INL and to photoreceptor cell bodies and their segments (**A**–**C**). In addition, PKM2 is associated with terminals in the IPL (**A**, **B**) and to astrocytes ([**A**, **B**, **D**] *arrows*). Pyruvate kinase M2 is not associated with RGC axons in the nerve fiber layer of the retina or the optic nerve (**D**–**F**) but is localized to cells with the morphology of astrocytes (**D**–**F**). Pyruvate kinase M2 is not expressed by extraocular muscle (**G**). In the brain, PKM2 is associated with astrocytes in gray matter ([**H**] *arrows*) and white matter ([**I**] *arrows*). *Scale bars*: 50 μm (**A**), 25 μm (**B**–**I**).

expressed by neurons in the outer part of the INL, a finding that might be expected given the presence of PKM1 in these cells in the marmoset (Fig. 4); second, PKM2 was weakly but unambiguously associated with Müller cells (Figs. 4, 7; Supplementary Fig. S6). In order to shed light on PKM isoenzyme expression in cones, we examined distributions of PKM1 and PKM2 in the cone-rich parafovea of the marmoset. Data showed robust expression of both PKM1 and PKM2 by cone axons in Henle's fiber layer by photoreceptor somata and by cone inner segments, whereas double-labeling experiments showed that both isoenzymes colocalized with the cone marker peanut agglutinin (Figs. 7D–H).

Quaternary Forms of PKM2 in Retina. Structurally, both PKM1 and PKM2 exist as homotetramers, configurations which favor glycolytic flux. A major functional difference between PKM1 and PKM2, however, is that the latter isoform harbors a binding site for fructose-1,6-bisphosphate, which serves as an allosteric modulator and causes the PKM2 tetramer to dissociate to a dimer. Dimeric PKM2 is much less efficient at converting phosphoenolpyruvate to pyruvate, and its presence therefore slows the rate of glycolytic flux; the resultant accumulation of upstream glycolytic intermediates are then available for use in anabolic reactions. The presence of a dimeric form of PKM2 within a cell, therefore, implies a reduced rate of glycolysis and an increased level of biosynthesis derived from glycolytic intermediates. With this in mind, we analyzed the relative levels of quaternary forms of PKM2 in the rat retina using a crosslinking protein-immunoblotting approach. This clearly resolved the monomeric protein at the expected molecular weight (~60 kDa). In retinal samples subjected to the cross-linking reaction, protein species were also present at molecular masses which corresponded to both dimeric (~120 kDa) and tetrameric (~240 kDa) forms (Fig. 8).

Lactate Dehydrogenase A

Validation of Antibodies. Two commercial antibodies, raised against human LDH-A (Supplementary Table S1), clearly recognized a protein of the expected size (~35 kDa) by Western blotting in skeletal muscle and liver (positive control tissues) as well as retina, optic nerve and brain. Both antibodies provided high signal to noise, cell-specific immunolabeling in mouse, rat, rabbit, monkey, and human tissue sections, including staining of extraocular muscle (positive control), while incubation with preimmune serum alone also elicited no signal. The patterns of immunolabeling of the two antibodies were alike. Thus, it can be concluded that in all species, the data generated are specific to LDH-A (Figs. 9, 10, 11, 12; Supplementary Fig. S7).

mRNA and Protein Expression and Immunolocalization. Lactate dehydrogenase A was expressed in large amounts in retina of mice and rats, with cycle thresholds of ~18 cycles. There was an approximately 2.5-fold greater expression of LDH-A mRNA in rat and mouse retinas than in cortex after

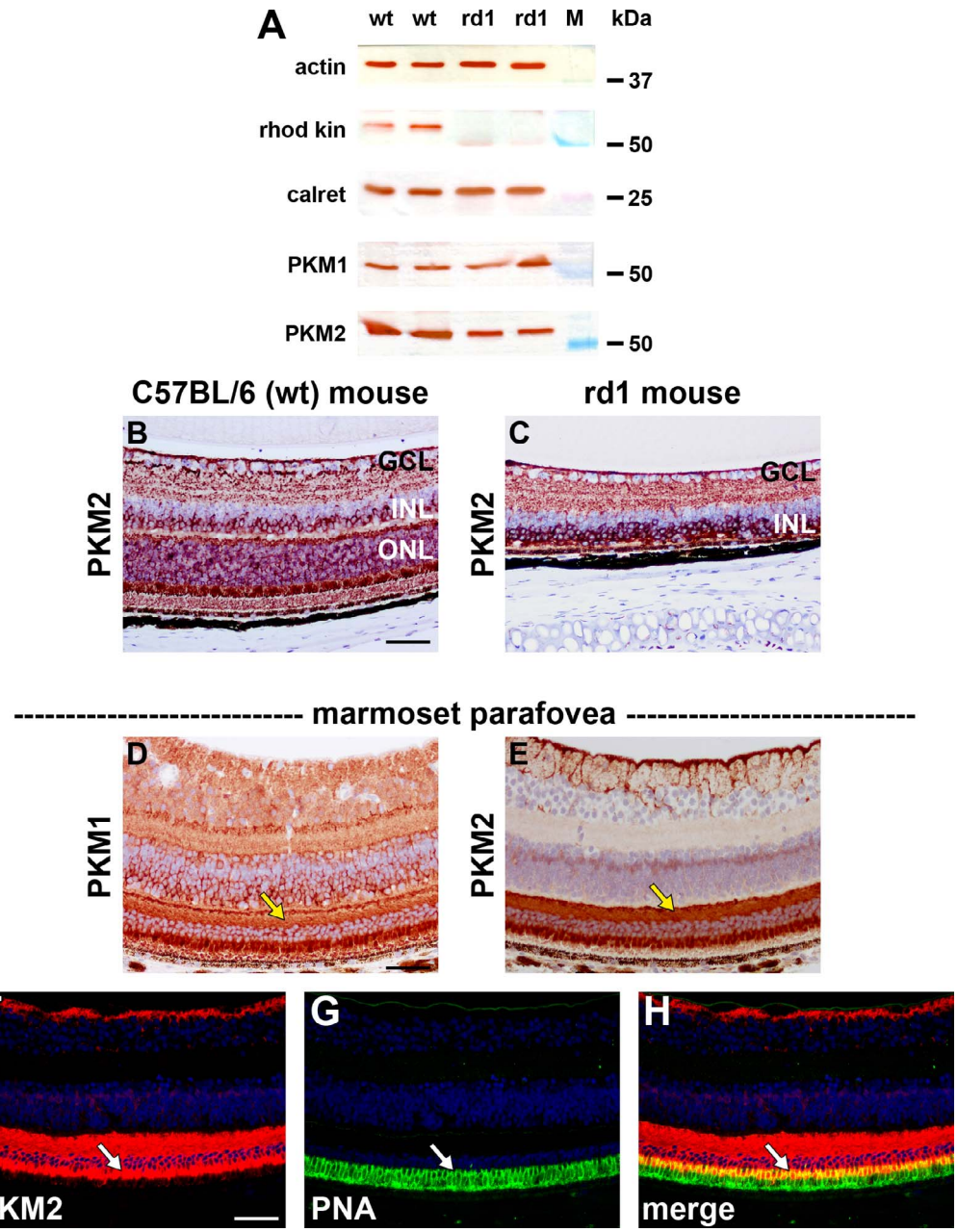

FIGURE 7. Analysis of PKM2 expression in mice lacking photoreceptors and in parafovea of the marmoset. (**A**) Retinal extracts from 8-week-old C57BL/6 (wild-type [wt]) and age-matched rd1 mice were probed for actin, rhodopsin kinase (rhod kin), calretinin (calret), PKM1, and PKM2 by Western blotting. Note the absence of rhodopsin kinase and the relatively lower level of PKM2 in Rd1 retinas. (**B**, **C**) Representative images of PKM2 immunolabeling in mouse retinas from 8-week-old C57BL/6 wt and age-matched rd1 mice. Both retinas display identical patterns of immunolabeling, except that rd1 mice lack a photoreceptor layer. (**D**, **E**) Representative images of PKM1 and PKM2 immunolabeling in the marmoset parafovea. Positive labeling is associated with cone axons in Henle's fiber layer (*yellow arrows*), photoreceptor somata in the outer nuclear layer, and cone inner segments. Double labeling immunofluorescence showed that PKM2 colocalized with the cone marker peanut agglutinin in inner segments ([**D**–**H**] *white arrows*). *Scale bars*: 25 μm. PNA, peanut agglutinin lectin.

normalization by GAPDH (Table 1). Consistent with this pattern, LDH-A protein, as detected by Western blotting, was more highly expressed in retina than in cortex (Fig. 9). Analysis of retina and optic nerve samples from four rats and mice revealed LDH-A expression in all samples but much fainter bands in the optic nerve samples (Fig. 9B; Supplementary Fig. S7).

The distribution of LDH-A in rodent retina paralleled that of PKM2 in many respects. Thus, in both rats (Fig. 10) and mice (data not shown), robust labeling of LDH-A was evident in photoreceptor cell bodies and their inner and outer segments. Lactate dehydrogenase A was likewise associated with bipolar cell bodies in the INL, together with their terminals in the IPL (Figs. 10, 11A–C). Lactate dehydrogenase A also did not colocalize with S100-positive Müller cells (Figs. 11A–C). Double labeling of PKM2 and LDH-A revealed the expected colocalization in photoreceptors and bipolar cells (Figs. 11G–I). Unlike PKM2, weak LDH-A immunoreactivity was associated with some cells, putatively amacrine cells, in the inner part of the INL.

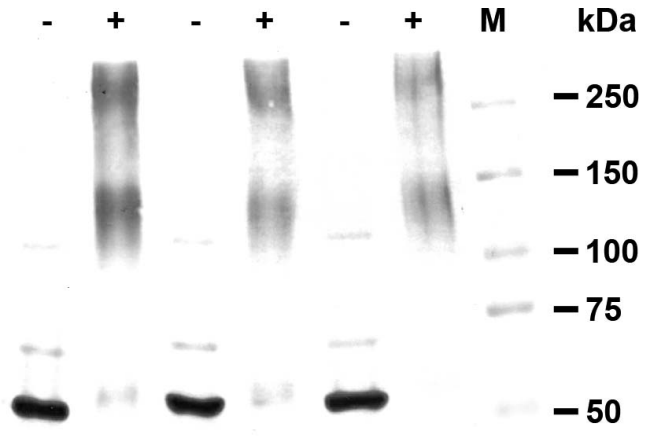

FIGURE 8. Relative levels of quaternary forms of PKM2 in rat retina, determined by using a cross-linking protein-immunoblotting approach (see Methods). Three individual retina homogenates were each split into 2 equal parts; 1 part was treated with the cross-linking reagent DSS (+), while the other was treated with vehicle (–). In vehicle-treated samples, there was clear resolution of monomeric PKM2 at the expected molecular weight (~60 kDa). In retinal samples subjected to the cross-linking reaction, protein species were also present at molecular masses that corresponded to both dimeric (~120 kDa) and tetrameric (~240 kDa) forms of PKM2.

Moreover, unlike PKM2, LDH-A did not localize to retinal or optic nerve astrocytes (Fig. 10). In the optic nerve, LDH-A expression was low with minimal expression by glial cells and indeterminate labeling of axons (Fig. 10).

In the marmoset retina (Fig. 12), LDH-A was very strongly expressed by photoreceptor cell bodies and their segments. Lactate dehydrogenase A labeling was also associated with a population of cells in the central part of the INL. These cells are not Müller cells as LDH-A failed to colocalize with CRALBP-positive Müller cells. Finally, weak LDH-A immunoreactivity was detectable in the GCL. In the optic nerve, LDH-A was not associated with glial cells, but axon bundles were lightly stained. The pattern of LDH-A immunolabeling in the human retina and optic nerve was similar to that observed in the marmoset, although the GCL and nerve fiber layer were more robustly labeled (Fig. 12).

PKM1, PKM2, and LDH-A Expression in Avascular Retina

As a final experiment, we investigated distribution patterns of LDH-A, and PKM1 and -2 in rabbit. Unlike rodents or primates, the rabbit has an avascular retina. Any differences between the vascular and avascular retina will impart a valuable perspective to the role of PKM and LDH-A in the retina. Data showed that distribution patterns of PKM1 in the avascular rabbit retina was analogous to those described in vascular retinas, namely expression by inner retinal neurons, photoreceptors, and axonal fibers in the optic nerve but negligible association with retinal or optic nerve glia (Supplementary Fig. S8). The distribution of PKM2 also displayed similarities in both avascular and vascular tissues, namely expression by photoreceptors and retinal and optic nerve glia. Nevertheless, PKM2 appears to be somewhat more abundant in the inner retina, notably Müller cell processes, of the rabbit and slightly less abundant in the outer retina compared to vascular retinas (Supplementary Fig. S8). The distribution of LDH-A showed the most marked dissimilarity between vascular and avascular retinas, being abundant in neurons and glia in the inner retina,

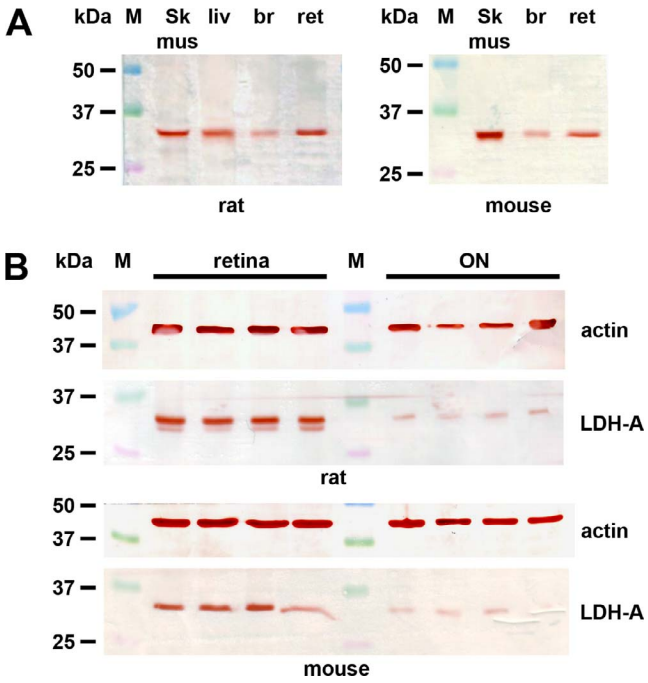

FIGURE 9. Western blot analysis of LDH-A expression in rat and mouse tissues. (**A**) Skeletal muscle (sk mus), liver (liv), brain (br), and retina (ret) tissue extracts probed for LDH-A. Note the lower level of LDH-A in brain samples. (**B**) Evaluation of LDH-A expression in retina (lanes 1–4) and optic nerve (lanes 6–9) tissue extracts obtained from 4 different rats and 4 different mice. Lactate dehydrogenase A is detectable in all samples but in much greater amounts in the retina.

but seemingly lacking in rod photoreceptors (Supplementary Fig. S8).

DISCUSSION

The current study has demonstrated that PKM2 is abundantly expressed in the photoreceptors of mammalian species including humans. Our findings complement those of Lindsay et al.,[14] who likewise showed expression of PKM2 by rodent photoreceptors. The PKM2 and LDH-A expression profile of photoreceptors is typical of proliferating normal and neoplastic cells rather than terminally differentiated neurons. The metabolic implication of this isoenzyme pattern is that the cell has both large energy and biosynthesis demands that can only be met by a high glycolytic rate even in the presence of oxygen. To our knowledge, retinal photoreceptors are the only nondividing adult cell type to display this pattern.

There are four known isoforms of PK in mammalian cells encoded by two genes, *PKLR* and *PKM*. PKLR is expressed in the liver and erythrocytes. The PKM isoforms PKM1 and PKM2 are alternative splice products of the *PKM* gene. Christofk et al.[22] reported that the switch from expression of physiological PKM1 to PKM2 in cancer cells was responsible for the Warburg effect. However, Bluemlein et al.[23] undermined this conclusion by using proteomics to definitively show that PKM2 was present in tumors and normal control tissue. Subsequently, Luo et al.[24] combined these observations into a coherent explanation by reporting that the Warburg effect in cancer (HeLa) cells was mediated via PKM2 serving as a coactivator of hypoxia-inducible factor-1α (HIF-1α). They showed that prolyl hydroxylation of PKM2 promotes the interaction of PKM2 with HIF-1α, thereby stabilizing HIF-1α binding to the hypoxia response elements of target genes, including LDH-A. They suggested that

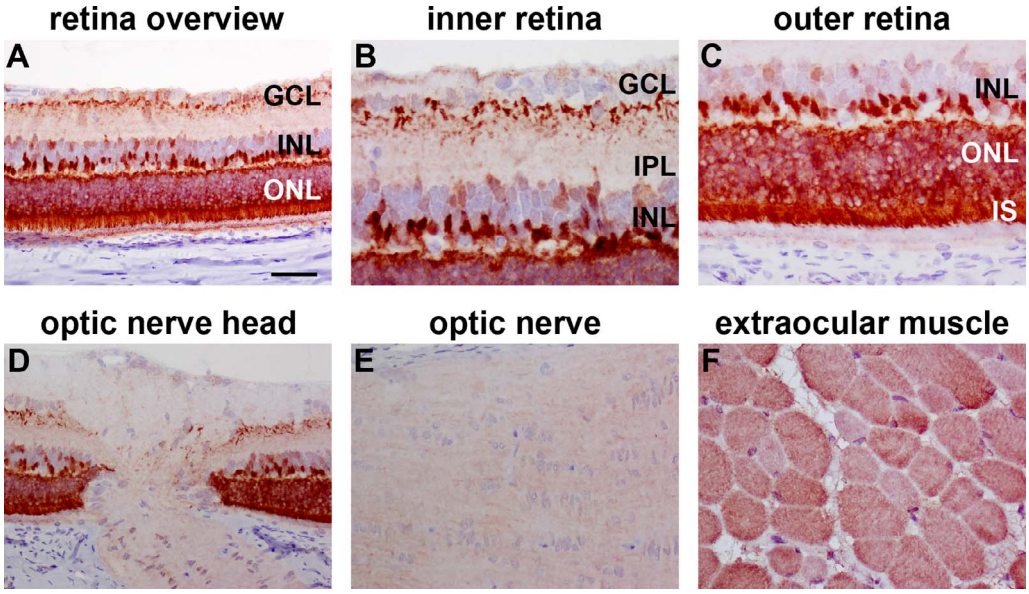

FIGURE 10. Representative images of LDH-A immunolabeling in rat retina and optic nerve. In the retina (**A**–**C**), positive labeling for LDH-A is localized to a population of cells, putatively bipolar cells, in the outer part of the INL together with terminals in the IPL. Lactate dehydrogenase A is also strongly expressed by photoreceptor cell bodies and their segments. Finally, weaker LDH-A labeling is associated with some cells in the inner part of the INL. Lactate dehydrogenase A is not localized to retinal astrocytes (**A**, **B**, **D**). In the optic nerve (**D**, **E**), LDH-A expression is low with minimal expression by axons and glial cells. As expected, LDH-A is expressed by extraocular muscle (**F**). *Scale bars*: 50 μm (**A**, **D**), 25 μm (**B**, **C**).

these molecules are not expressed together under physiological conditions in most tissues but occur in cancers due to the frequent presence of hypoxia and/or other HIF stabilization factors. Recent studies have demonstrated that PKM2 has nonmetabolic, epidermal growth factor–dependent actions that can promote tumorigenesis and the Warburg effect in certain cancer cell lines.[25–27] Other factors, particularly the oncogene c-Myc for which PKM2 can also serve as a transcriptional coactivator, are also mediators of the Warburg effect in some neoplastic cells. However, the emerging evidence indicates that PKM2 is a master regulator of the Warburg effect in cancer.[28,29]

With occasional exceptions,[30,31] cancer research reports are replete with references to PKM2 as "tumor specific" or as representing the "oncofetal" form of PK, which is replaced by PKM1 in adult tissue, despite the original report of PK isoenzymes demonstrating PKM2 in normal adult tissues (the retina was not studied),[32] and the recent report by Bluemlein et al.[23] demonstrating PKM2 in normal adult control tissues. Clearly, PKM2 is not tumor-specific. Recent strategies to target PKM2 as a novel cancer therapy[33] should proceed cautiously and at least include ophthalmic assessment in phase I trials.[34]

Although the changing quaternary structure of PKM2 regulates the flow of glycolysis and is under allosteric control by upstream glycolytic intermediates[12] and serine,[13] provided the cell has pyruvate, the catalytic activity of PKM2 is theoretically not a fundamental requirement for the Warburg effect (the production of lactate under aerobic conditions). Conversion of pyruvate to lactate in the cytosol rather than the entry of pyruvate into mitochondria, despite the presence of oxygen, is the fundamental requirement. Hence, biosynthesis demands are a plausible explanation but not a logical necessity for the existence of the Warburg effect. In fact, recent mathematical modeling that accounts for space limitations within the cell (and the large volume occupied by mitochondria relative to glycolytic enzymes) finds that a high glycolytic rate optimizes ATP production when glucose is abundant.[35] This finding explains the presence of the Warburg effect with glycolytic ATP production (and lactate production) in highly active skeletal muscle (which does not contain PKM2) when oxygen is not limiting.[36] The factors forcing conversion of pyruvate to lactate in this situation are not clear. Although cellular biosynthesis and PKM2 are not fundamental requirements for the Warburg effect, the convergence of evidence indicates that PKM2 has important roles in regulating the Warburg effect in cells with large biosynthesis and energy demands.

Pyruvate kinase M1 was confined to neurons and axons in the retina and brain in a pattern consistent with nonproliferating cells with a predominantly aerobic metabolism. X-ray crystallography has demonstrated that PKM1 exists as pairs of active dimers[37]; however, the isoform is not under allosteric control by glycolytic intermediates.[12] In contrast, PKM2 is believed to exist as an active tetrameric form and a relatively inactive dimeric form, termed M2-PK.[38] The presence of the dimeric form of PKM2 within a cell implies a reduced rate of glycolysis and an increased level of biosynthesis derived from glycolytic intermediates. Antibodies to "tumor M2-PK" are commercially available and are used in diagnostic testing of cancer; however, to our knowledge, the specificity of this antibody to the proposed dimeric form has not been validated. In our hands, tumor M2-PK antibody yielded data that are consistent with the antibody binding nonselectively to both PKM1 and PKM2 (data not shown). With this in mind, we investigated the quaternary forms of PKM2 in the rat retina using a crosslinking protein-immunoblotting approach. Using this methodology, we clearly demonstrated the dimeric form in retina. Hence, it seems likely that PKM2 is under allosteric control by fructose-1,6-biphosphate in the mammalian retina in a similar manner to proliferating tissue.[12]

As well as photoreceptors, PKM2 also colocalized with bipolar cells in the rodent retina and astrocytes in the retina, optic nerve, and brain. Interestingly, we could not demonstrate either PKM1 or PKM2 localization to retinal Müller cells in rats or mice. Our data are consistent with those of recent findings by Lindsay et al.,[14] who observed the same phenomenon in mice. In a comprehensive series of experiments they described novel metabolic pathways between retinal neurons and Müller

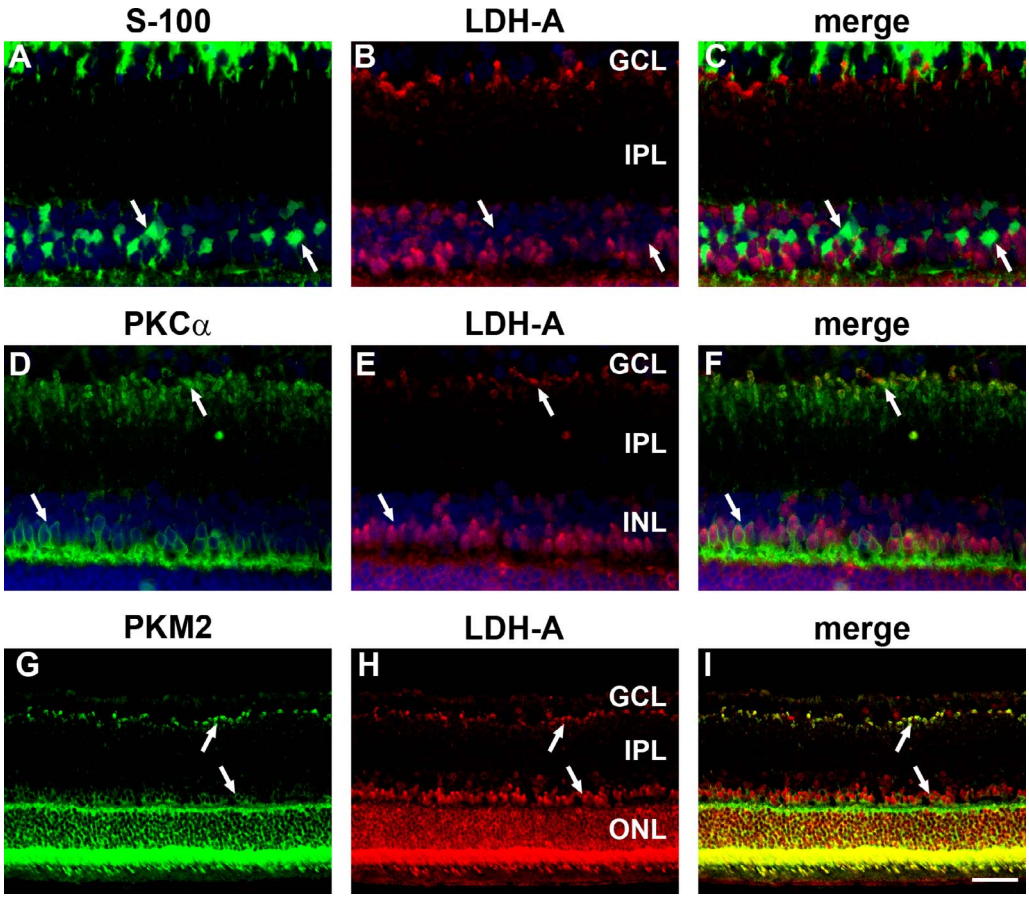

Figure 11. Double labeling immunofluorescence of LDH-A in rat retina. Lactate dehydrogenase A is not associated with S100-positive Müller cells ([**A–C**] *arrows*). In contrast, LDH-A colocalizes with some PKCα-positive bipolar cell bodies in the INL and their terminals adjacent to the GCL ([**D–F**] *arrows*). Expression of LDH-A overlaps considerably with that of PKM2, with colocalization in photoreceptors as well as in bipolar cell bodies and their terminals ([**G–I**] *arrows*). *Scale bars*: 25 μm (**A–F**); 50 μm (**G–I**).

cells deficient in pyruvate kinase.[14] However, our results show that PKM2 is expressed by Müller cells in marmosets, albeit at a considerably lower level than in photoreceptors, suggesting species differences in Müller cell metabolism. An evolutionary difference was also apparent with regard to bipolar cells: PKM2 was present in rodent bipolar cells, but primate bipolar cells expressed PKM1. The biosynthesis demands of the bipolar cells are likely to be less than the photoreceptors, and unlike astrocytes bipolar cells do not have the capacity to proliferate. Accordingly, an explanation for why rodent bipolar cells have a glycolytic enzyme pattern that is different to the pattern found in brain neurons and inner retinal neurons (amacrine cells, retinal ganglion cells) is not immediately apparent.

A limitation of the current study is that we did not obtain data at different times during the light/dark cycle. Hence, we have a static picture of the isoenzyme pattern. It is possible that this pattern or relative amounts of isoenzyme would fluctuate with disc shedding rates.[39] However, Lindsay et al.[14] recently reported that the pattern of PKM2 expression in mice was not affected by light; thus, it appears unlikely that a major diurnal change exists.

Lactate dehydrogenase is a tetrameric enzyme comprising two major subunits A and/or B, (encoded by the *Ldh-A* and *Ldh-B* genes, respectively) resulting in five isoenzymes (A4, A3B1, A2B2, A1B3, and B4) that catalyze the forward and backward conversion of pyruvate to lactate. Lactate dehydrogenase A (LDH-5, M-LDH, or A4) is the predominant form in skeletal muscle. Lactate dehydrogenase B (LDH-1, H-LDH, or B4) is found in heart muscle. Lactate dehydrogenase was one of the first enzymes recognized to have different isoforms,[40] and since their discovery, they have been conceptualized as having different physiological roles based on different enzyme kinetics: LDH-A predominantly catalyzing pyruvate to lactate, and critical for the Warburg effect, and LDH-B catalyzing the reverse reaction and predominating in well-oxygenated tissues. Lactate dehydrogenase enzyme kinetics have been widely studied, but reports are inconsistent, and simplistic notions that their kinetics affect physiological roles at equilibrium have recently been challenged.[41] However, under conditions of high glycolytic flux, varying kinetics are likely to significantly affect function,[41] and it would appear that LDH-A is a *sine qua non* for the Warburg effect.

In 1964, Graymore[42] noted that the expression of the LDH-A isoenzyme in the retina was reduced in rats with inherited "retinitis pigmentosa," characterized pathologically by loss of the photoreceptors. This observation was interpreted to imply that the photoreceptors were principally responsible for the retinal lactate production. This supported earlier evidence that the photoreceptors were particularly susceptible to glycolytic inhibition.[8] Similarly, Acosta et al.[43] demonstrated a high expression of LDH-A in mouse retina, in contrast to the minimal expression in brain. They noted that the high expression rate was lost in *rd1* mice after the onset of photoreceptor degeneration.[43] These observations were drawn from immunoblots, and almost all metabolic evidence for the

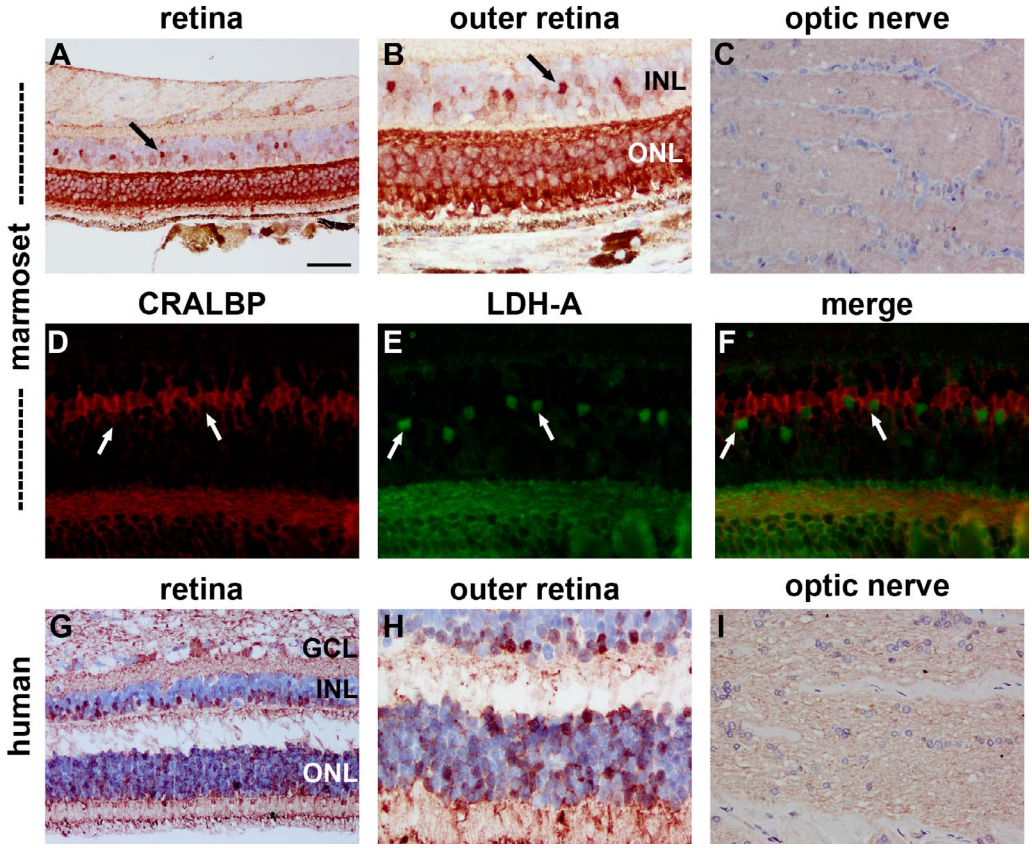

Figure 12. Representative images of LDH-A immunolabeling in marmoset and human retina and optic nerve. In marmoset retina, LDH-A is strongly expressed by photoreceptor cell bodies and their segments (**A**, **B**). Lactate dehydrogenase A labeling is also associated with a population of cells in the central part of the INL ([**A**, **B**] *black arrows*). These cells are not Müller cells as LDH-A fails to colocalize with CRALBP ([**D–F**] *white arrows*). Weak LDH-A immunoreactivity was detectable in the GCL (**A**). In the optic nerve, LDH-A was not associated with glial cells, but axon bundles were weakly positive (**C**). The pattern of LDH-A immunolabeling in the human retina and optic nerve was similar to that observed in the marmoset, although the GCL and nerve fiber layer were more robustly labeled (**G–I**). *Scale bars*: 50 μm (**A**, **C**, **G**, **I**), 25 μm (**B**, **D–F**, **H**).

Warburg effect in the retina comes from experiments on whole retinas, with no discrimination between the different retinal layers. Researchers have obtained some information about the relative glycolytic versus oxidative phosphorylation contribution of the outer retina compared to the inner retina from electrophysiological studies in the presence of retinal ischaemia,[4,44,45] but an understanding of retinal metabolism remains far from complete. Our results indeed confirm the hypothesis that photoreceptors express high levels of LDH-A. This was true for all species analyzed. Lactate dehydrogenase A, however, was not restricted to photoreceptors. Other neuronal classes, such as bipolar cells and, to a lesser degree, amacrine cells were also LDH-A-positive in certain species. In contrast, neither astrocytes nor Müller cells were associated with LDH-A immunolabeling in any species, suggesting that neither of these cell types produce significant quantities of lactate. Similarly in the optic nerve, LDH-A was not expressed by astrocytes or oligodendrocytes.

To impart perspective to our results, we explored the distribution patterns of LDH-A and PKM1 and -2 in the rabbit. Unlike rodents or primates, the rabbit has an avascular retina. Moreover, glycogen storage is abundant in the inner layers of the rabbit retina, and particularly concentrated in Müller cells, but is very limited in the rat or mouse.[46] Our results showed some discrepancies between avascular and vascular retinas, most notably concerning LDH-A, which was abundant in the inner retina but sparse in rod photoreceptors of the rabbit, results contradictory to those obtained in vascular retinas. These data agree with those of Ames et al.,[47] who investigated the energy requirements of the rabbit retina and concluded

Table 2. Relative Levels of PKM1, PKM2, and LDH-A Immunolabeling in Different Cell Rodent and Primate Populations

	Rodent			Primate		
Tissue	**PKM1**	**PKM2**	**LDH-A**	**PKM1**	**PKM2**	**LDH-A**
Inner retinal neurons	+++	+	+	+++	++	+
Photoreceptors	++	+++	+++	++	+++	+++
Retinal glia	–	+	–/+	–	++	–/+
Brain neurons	+++	–	ND	+++	–	ND
Brain glia	–	++	ND	–	++	ND

ND, not determined.

that the inner retina was supported almost entirely by anaerobic glycolysis to lactate, whereas the outer retina was normally supported by oxidative metabolism. Our results are also consistent with those of Poitry-Yamate et al.,[48] who showed that in the avascular guinea pig retina, Müller cells produce lactate that is released and metabolized by photoreceptors. Overall, then, it appears that in the avascular inner retina, the abundant supply of glycogen is metabolized to lactate via LDH-A, whereas the photoreceptors have minimal LDH-A and therefore likely do not produce lactate themselves. In contrast, in the vascular retina, photoreceptors have a high glycolytic rate and produce large quantities of lactate, presumably via their high level of LDH-A, whereas the inner retina is largely oxidative.

In conclusion, we characterized the cell-specific localization of PKM1, PKM2, and LDH-A in the retina of five mammalian species. An overview of the relative levels of PKM1, PKM2, and LDH-A immunolabeling in the different cell rodent and primate populations is shown in Table 2. The most striking finding was the consistently high expression of PKM2 in the photoreceptors across all species in a pattern similar to that reported in neoplastic tissue. Gardner et al.[49] recently showed the importance of glycolysis in retinal protein synthesis and uncovered an interaction between glycolysis and Akt/mTOR-regulation of anabolic pathways. Although Lindsay et al.[14] found no incorporation of radiolabelled glucose into serine in murine retinal explants over a 6-hour period, we propose that the prodigious biosynthesis requirements associated with in vivo disc shedding and turnover of opsin underpin the isoenzyme pattern we have observed. The cellular requirement for both energy and biomass production would explain the existence of the Warburg effect in the photoreceptors. Our findings suggest that photoreceptor metabolism may use PKM2 as the "molecular switch" between energy production and biomass production. The presence of PKM2 in rod photoreceptors of the avascular retina supports this hypothesis, but the relative lack of LDH-A in the same cell type casts some doubt on the universal requirement of aerobic glycolysis for photoreceptor homeostasis.

Acknowledgments

Supported by National Health and Medical Research Council Grant 626964 and the Ophthalmic Research Institute of Australia. The authors alone are responsible for the content and writing of the paper.

Disclosure: **R.J. Casson**, None; **J.P.M. Wood**, None; **G. Han**, None; **T. Kittipassorn**, None; **D.J. Peet**, None; **G. Chidlow**, None

References

1. Ng SK, Wood JP, Chidlow G, et al. Cancer-like metabolism of the mammalian retina. *Clin Experiment Ophthalmol*. 2015;43:367–376.
2. Wong-Riley MT. Energy metabolism of the visual system. *Eye Brain*. 2010;2:99–116.
3. Young RW. The renewal of photoreceptor cell outer segments. *J Cell Biol*. 1967;33:61–72.
4. Winkler BS. Glycolytic and oxidative metabolism in relation to retinal function. *J Gen Physiol*. 1981;77:667–692.
5. Wind F. *The Metabolism of Tumors: Investigations from the Kaiser Wilhelm Institute for Biology.* Warburg O, ed. Berlin-Dahlem: Constable & Co. Ltd., 1930;282.
6. Graymore C, Tansley K. Iodoacetate poisoning of the rat retina. II. Glycolysis in the poisoned retina. *Br J Ophthalmol*. 1959;43:486–493.
7. Graymore C, Tansley K. Iodoacetate poisoning of the rat retina. I. Production of retinal degeneration. *Br J Ophthalmol*. 1959;43:177–185.
8. Noell WK. The impairment of visual cell structure by iodoacetate. *J Cell Physiol*. 1952;40:25–55.
9. Miao P, Sheng S, Sun X, Liu J, Huang G. Lactate dehydrogenase A in cancer: a promising target for diagnosis and therapy. *IUBMB Life*. 2013;65:904–910.
10. Vander Heiden MG, Cantley LC, Thompson CB. Understanding the Warburg effect: the metabolic requirements of cell proliferation. *Science*. 2009;324:1029–1033.
11. Mazurek S. Pyruvate kinase type M2: a key regulator of the metabolic budget system in tumor cells. *Int J Biochem Cell Biol*. 2011;43:969–980.
12. Jurica MS, Mesecar A, Heath PJ, Shi W, Nowak T, Stoddard BL. The allosteric regulation of pyruvate kinase by fructose-1,6-bisphosphate. *Structure*. 1998;6:195–210.
13. Chaneton B, Hillmann P, Zheng L, et al. Serine is a natural ligand and allosteric activator of pyruvate kinase M2. *Nature*. 2012;491:458–462.
14. Lindsay KJ, Du J, Sloat SR, et al. Pyruvate kinase and aspartate-glutamate carrier distributions reveal key metabolic links between neurons and glia in retina. *Proc Natl Acad Sci U S A*. 2014;111:15579–15584.
15. Morohoshi K, Ohbayashi M, Patel N, Chong V, Bird AC, Ono SJ. Identification of anti-retinal antibodies in patients with age-related macular degeneration. *Exp Mol Pathol*. 2012;93:193–199.
16. Chidlow G, Daymon M, Wood JP, Casson RJ. Localization of a wide-ranging panel of antigens in the rat retina by immunohistochemistry: comparison of Davidson's solution and formalin as fixatives. *J Histochem Cytol*. 2011;59:884–898.
17. Chidlow G, Holman MC, Wood JP, Casson RJ. Spatiotemporal characterization of optic nerve degeneration after chronic hypoperfusion in the rat. *Invest Ophthalmol Vis Sci*. 2010;51:1483–1497.
18. Chidlow G, Wood JP, Casson RJ. Expression of inducible heat shock proteins Hsp27 and Hsp70 in the visual pathway of rats subjected to various models of retinal ganglion cell injury. *PLoS One*. 2014;9:e114838.
19. Chidlow G, Wood JP, Manavis J, Osborne NN, Casson RJ. Expression of osteopontin in the rat retina: effects of excitotoxic and ischemic injuries. *Invest Ophthalmol Vis Sci*. 2008;49:762–771.
20. Haverkamp S, Wassle H. Immunocytochemical analysis of the mouse retina. *J Comp Neurol*. 2000;424:1–23.
21. Goldberg MS, Sharp PA. Pyruvate kinase M2-specific siRNA induces apoptosis and tumor regression. *J Exp Med*. 2012;209:217–224.
22. Christofk HR, Vander Heiden MG, Harris MH, et al. The M2 splice isoform of pyruvate kinase is important for cancer metabolism and tumour growth. *Nature*. 2008;452:230–233.
23. Bluemlein K, Gruning NM, Feichtinger RG, Lehrach H, Kofler B, Ralser M. No evidence for a shift in pyruvate kinase PKM1 to PKM2 expression during tumorigenesis. *Oncotarget*. 2011;2:393–400.
24. Luo W, Hu H, Chang R, et al. Pyruvate kinase M2 is a PHD3-stimulated coactivator for hypoxia-inducible factor 1. *Cell*. 2011;145:732–744.
25. Yang W, Xia Y, Hawke D, et al. PKM2 phosphorylates histone H3 and promotes gene transcription and tumorigenesis. *Cell*. 2012;150:685–696.
26. Yang W, Zheng Y, Xia Y, et al. ERK1/2-dependent phosphorylation and nuclear translocation of PKM2 promotes the Warburg effect. *Nat Cell Biol*. 2012;14:1295–1304.

Investigative Ophthalmology & Visual Science

27. Yang W, Xia Y, Ji H, et al. Nuclear PKM2 regulates beta-catenin transactivation upon EGFR activation. *Nature*. 2011;480:118–122.
28. Wang HJ, Hsieh YJ, Cheng WC, et al. JMJD5 regulates PKM2 nuclear translocation and reprograms HIF-1alpha-mediated glucose metabolism. *Proc Natl Acad Sci U S A*. 2014;111:279–284.
29. Filipp FV. Cancer metabolism meets systems biology: pyruvate kinase isoform PKM2 is a metabolic master regulator. *J Carcinogenesis*. 2013;12:14.
30. Chaneton B, Gottlieb E. Rocking cell metabolism: revised functions of the key glycolytic regulator PKM2 in cancer. *Trends Biochem Sci*. 2012;37:309–316.
31. Israelsen WJ, Vander Heiden MG. Pyruvate kinase: function, regulation and role in cancer. *Semin Cell Dev Biol*. 2015;43:43–51.
32. Imamura K, Tanaka T. Multimolecular forms of pyruvate kinase from rat and other mammalian tissues. I. Electrophoretic studies. *J Biochem (Tokyo)*. 1972;71:1043–1051.
33. Yang W, Lu Z. Regulation and function of pyruvate kinase M2 in cancer. *Cancer Lett*. 2013;339:153–158.
34. Ng SK, Wood JP, Chidlow G, Peet DJ, Casson RJ. Potential adverse effects to the retina of cancer therapy targeting pyruvate kinase M2. *Acta Oncol*. 2015;54:136–137.
35. Vazquez A, Oltvai ZN. Molecular crowding defines a common origin for the Warburg effect in proliferating cells and the lactate threshold in muscle physiology. *PLoS One*. 2011;6:e19538.
36. Kemper WF, Lindstedt SL, Hartzler LK, Hicks JW, Conley KE. Shaking up glycolysis: sustained, high lactate flux during aerobic rattling. *Proc Natl Acad Sci U S A*. 2001;98:723–728.
37. McPherson A Jr, Rich A. Preliminary x-ray study of rabbit muscle pyruvate kinase. *J Biol Chem*. 1972;247:1334–1335.
38. Eigenbrodt E, Leib S, Kramer W, Friis RR, Schoner W. Structural and kinetic differences between the M2 type pyruvate kinases from lung and various tumors. *Biomed Biochim Acta*. 1983;42:S278–S282.
39. LaVail MM. Rod outer segment disk shedding in rat retina: relationship to cyclic lighting. *Science*. 1976;194:1071–1074.
40. Markert CL. Lactate dehydrogenase isozymes: dissociation and recombination of subunits. *Science*. 1963;140:1329–1330.
41. Quistorff B, Grunnet N. The isoenzyme pattern of LDH does not play a physiological role; except perhaps during fast transitions in energy metabolism. *Aging*. 2011;3:457–460.
42. Graymore C. Possible significance of the isoenzymes of lactic dehydrogenase in the retina of the rat. *Nature*. 1964;201:615–616.
43. Acosta ML, Fletcher EL, Azizoglu S, Foster LE, Farber DB, Kalloniatis M. Early markers of retinal degeneration in rd/rd mice. *Mol Vis*. 2005;11:717–728.
44. Bui BV, He Z, Vingrys AJ, Nguyen CT, Wong VH, Fortune B. Using the electroretinogram to understand how intraocular pressure elevation affects the rat retina. *J Ophthalmol*. 2013;2013:262467.
45. Tsai TI, Bui BV, Vingrys AJ. Effect of acute intraocular pressure challenge on rat retinal and cortical function. *Invest Ophthalmol Vis Sci*. 2014;55:1067–1077.
46. Kuwabara T, Cogan DG. Retinal glycogen. *Arch Ophthalmol*. 1961;66:680–688.
47. Ames A III, Li YY, Heher EC, Kimble CR. Energy metabolism of rabbit retina as related to function: high cost of Na+ transport. *J Neurosci*. 1992;12:840–853.
48. Poitry-Yamate CL, Poitry S, Tsacopoulos M. Lactate released by Muller glial cells is metabolized by photoreceptors from mammalian retina. *J Neurosci*. 1995;15:5179–5191.
49. Gardner TW, Abcouwer SF, Losiewicz MK, Fort PE. Phosphatase control of 4E-BP1 phosphorylation state is central for glycolytic regulation of retinal protein synthesis. *Am J Physiol Endocrinol Metab*. 2015;309:E546–E556.

Investigative Ophthalmology & Visual Science